

Statistics of the Approach Process at Detroit Metropolitan Wayne County Airport

Babak G. Jeddi, John F. Shortle, Lance Sherry

Abstract—Dealing with uncertainty is a necessary and difficult aspect in operations analysis of complex systems such as the air transportation system. We represent these uncertainties in the approach process by probability distributions. This paper provides statistical observations of the approach and landing process at Detroit Metropolitan airport (DTW) for one week of February 2003. These probability distributions are based on aircraft track record data at DTW which are collected by a multilateration surveillance system. After explaining characteristics of the database and its short comings, we present a methodology to extract necessary statistical samples. From this, we obtain appropriate probability distributions for landing time interval (LTI), inter arrival distance (IAD), and runway occupancy time (ROT) presented under instrument flight rules (IFR) and peak traffic periods.

Index Terms—Aircraft approach, probability, risk, safety, stochastic processes

I. INTRODUCTION

UNDERSTANDING the stochastic behavior of the approach and landing process is critical to analyze runway separation risk and runway capacity. Statistical analysis is a method for this purpose. In recent years, multilateration systems have been installed in some airports, including Detroit Metropolitan Wayne County airport (DTW). These systems provide reasonably accurate time-position estimates of all transponder-equipped aircraft (a/c) operating in the airport vicinity in all weather conditions. These data can be used to obtain samples of landing process variables, such as the Landing Time Interval (LTI) between successive aircraft to the runway threshold, the Inter-Arrival Distance (IAD) between two successive aircraft at the moment that the lead aircraft crosses the runway threshold, and Runway Occupancy Times (ROT). ROT is the length of time required for an arriving aircraft to proceed from over the runway threshold to a point clear of the runway. This paper considers *LTI*, *IAD*, and *ROT* as (random) variables.

Manuscript received February 26, 2006. This work is supported in part by Wayne Bryant, Wake Program Manager, NASA Langley Research Center.

Babak G. Jeddi is a Ph.D. candidate in the Department of Systems Engineering and Operations Research at George Mason University, Fairfax, VA 22030 US (Corresponding author, Phone: +1 (703) 505-5994; fax: +1 (703) 993-1521; e-mail: BGhalebs@gmu.edu).

John F. Shortle is an assistant professor in the Department of Systems Engineering and Operations Research at George Mason University, Fairfax, VA 22030 US. (e-mail: JShortle@gmu.edu).

Lance Sherry is an associate research professor in the Department of Systems Engineering and Operations Research at George Mason University, Fairfax, VA 22030 US. (e-mail: LSherry@gmu.edu).

Levy *et al.* [1] use multilateration data of Memphis International airport (MEM) to obtain probability distributions of *LTI* and average landing speed conditioned on the type of follow-lead aircraft in visual meteorological condition (VMC).

Probability distributions for *LTI* and *ROT* are also estimated by Haynie [2] for Atlanta International airport (ATL) using his field observations from this airport. References [3]-[5] provide distribution fits for Haynie's observations, as well as field observations from LaGuardia airport (LGA). However, the sample sizes are small, and the results are not conditioned on aircraft weight class type, or heavy traffic times. Also, they have not obtained samples of *IAD*, which we provide here. Reference [6] provides analysis of *IAD*, *LTI*, and runway utilization in peak periods at Dallas/Fort Worth International Airport (DFW). They include both instrument meteorological condition (IMC) and VMC times in their study; however, they do not fit known specific probability distributions to the observations. They use radar data, which normally do not extend to the runway threshold, so they must extrapolate aircraft flight paths to the most likely runway threshold.

Vandevenne and Lippert [7] develop a model to represent *LTI* and provide a probability distribution fit. This model is the convolution of exponential and normal distributions. Andrews and Robinson [8] extend the capabilities used in [6]. They fit probability distribution functions for *LTI* using the Vandevenne and Lippert model [7]. Rakas and Yin [9] use Performance Data Analysis and Reporting System (PDARS) database to estimate probability distribution of *LTI* under VMC in Los Angeles International Airport (LAX). For this purpose, they develop a PDF which they name it *double-normal* distribution.

The Center for Air Transportation Systems Research (CATSR) at George Mason University (GMU) has access to multilateration surveillance system data of DTW via Volpe National Transportation Systems Center, an organization within the US Department of Transportation. The original multilateration data are de-identified by Sensis Corporation, and the filtered data are used in this study. However, as discussed later, there are still some outliers, noise, and missing data present in the database.

This paper introduces the characteristics and organization of available data and the algorithms that we have initiated to extract recorded data of landing times and position over the runway thresholds, runway exit times, and the position of the following aircraft when its lead crosses the runway threshold. Then this algorithm is used to investigate DTW data from Feb2, 2003 to Feb8, 2003 (in Greenwich Mean Time) in order to provide probability distributions for *LTI*, *IAD*, at runway thresholds, and *ROT*. Fig. 1 is a simplified diagram of this airport.

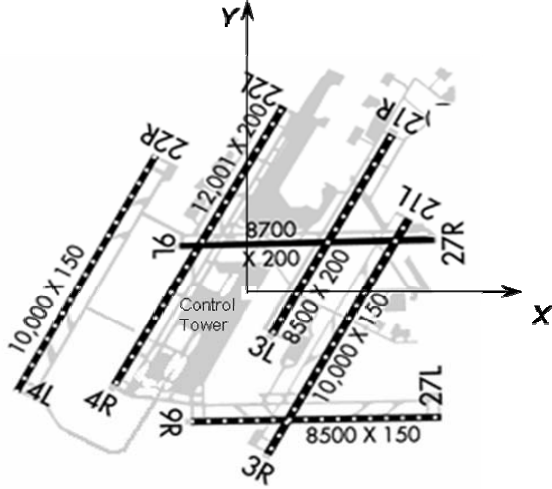


Fig. 1. Simplified DTW airport diagram (<http://www.airnav.com/airport/KDTW>)

We have organized this paper as follows. Section 2 provides details about the database structure, noise and outliers, and data preparation necessary to extract the required landing samples. Section 3 presents statistical findings and probability distribution fits for “peak traffic period landing variables” *LTI*, *IAD*, and *ROT*, under IMC. (In this paper, IMC is defined by the IMC / VMC flag in the ASPM database, which provides conditions at the airport.) Section 4 presents conclusions of the study and some topics for future research.

II. DATABASE STRUCTURE AND SAMPLE EXTRACTION PROCEDURE

Multilateration data must be processed to perform probabilistic analysis of the operations. There are two categories of short comings with the data. First, the data contain noise, outliers, and missing records, and second, the data provide the aircraft time-position tracks but do not specify when aircraft cross certain positions. In this section, we discuss these problems and explain our strategy to extract necessary samples for statistical analysis of the approach process.

We make use of five fields from the multilateration data (out of a possible eighteen): aircraft mode-s, time (t in seconds), longitude (X in meters), latitude (Y in meters), and mode-c. The mode-s field is a number of an attached transponder that uniquely identifies an aircraft. The transponder is generally attached somewhere close to the center of the aircraft. The mode-c field is a barometer-based value that can be converted to altitude (in feet) by multiplying it by 25 and adding 10,000 to the result. However, the obtained value is not very reliable for this purpose due to pressure change and barometer errors under for different weather conditions. Time and position of aircraft are recorded every second. For the week Feb 2, 2003 to Feb 8, 2003, the database includes 33,030,878 records, requiring 1GB of disk space.

A. Data preparation

The database is in Oracle format and we use SQL+ to

obtain queries. Necessary manipulations and sample extractions are done in MATLAB.

To start, we sort the Oracle data by mode-s and then by time. We also change the time stamp to the format “dd/mm/yy hh:mi:ss.” Basic queries demonstrated that the mode-s is missing for some records. In some cases, the mode-s of an entire aircraft track is missing. In other cases, we are missing the mode-s of only a few points along a track. We eliminate all of these data points. In the latter case, we retain the basic track path, since we can linearly interpolate the path of the aircraft from the other points with mode-s. In the former case, we discard the entire track. This may result in some inter-arrival times that are too long. However, because of the available data, losing some possible landing records does not significantly influence the study.

In the database, the origin ($X=0, Y=0$) of the Euclidian coordinate is the FAA control tower located between runways 21R and 22L, as shown in Fig. 1, and the Y axis indicates the true north. Runway 21L, and all other runways parallel to it, have a Magnetic angle of 214.8° . True North and Magnetic North have an angle of 6.1° W, as indicated in airport diagram [10]. Thus, the true angle of runway 21L is $214.8 - 6.1 = 208.7^\circ$, or equivalently 61.3° from the X-axis. Since data are collected in the true coordinates, we observe the same results by tracking the aircraft course on the runways [11]. In the same manner, we calculate the true angle of runways 27L/09R and 27R/09L as 1.3° from the X-axis.

To simplify working with the database, we rotate coordinates to make the runways parallel to the X-axis. To find the aircraft position in the rotated coordinates we multiply the observed (X, Y) position by the rotation matrix R as

$$R = \begin{pmatrix} \cos(a) & \sin(a) \\ -\sin(a) & \cos(a) \end{pmatrix}, \quad (1)$$

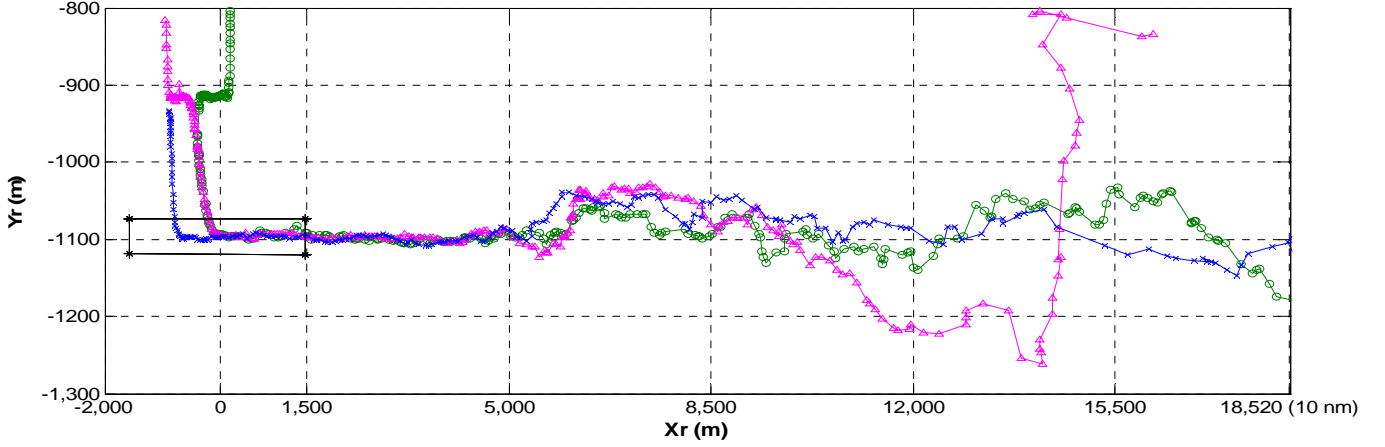
where a is the rotation angle which is 61.3° for runways 21L/03R, 21R/03L, 22L/04R and 22R/04L, and 1.3° for runways 27L/09R and 27R/09L as described before. That is, the aircraft position in the rotated Euclidian coordinates is

$$\begin{pmatrix} X_r \\ Y_r \end{pmatrix} = R * \begin{pmatrix} X \\ Y \end{pmatrix}. \quad (2)$$

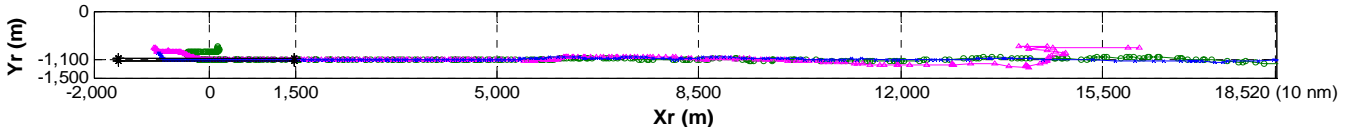
Using the rotation formula (2), we also transform the runway coordinates to the new coordinates.

Preliminary queries and plots demonstrated some noise in the data. Fig. 2 is the ground projection (bird’s eye view) of the track plot of sample aircraft landings on runway 21L. Fig. 2a (the lower figure) is drawn to scale, whereas Fig. 2b is expanded in the Y_r -axis. In the figure, two aircraft exit the runway from the high-speed exit located after the middle of the runway. Based on visual investigation, the noise of X - Y positions is assumed to be in an acceptable range, for a given time, as demonstrated in Fig. 2b. In frequent cases, there are two or more records of a given aircraft at the same second. We average the records in such cases.

Since landings are the subject of study, it is sufficient to



a) Exaggerated in Yr axis



a) Drawn to scale

Fig. 2 (a) Landing and exit track of three large a/c on/from runway 21L, (b) exaggerated version of figure (a) in Yr axis

consider data in a rectangle, which we call the “query box.” The sides of the query box are parallel to the sides of the runway rectangle, and the box includes the runway and the common landing path extended about 10 nm from the runway threshold. For runway 21L, for example, we consider the rectangle $-1350\text{m} < X_r < 18500\text{m}$, and $-3000\text{m} < Y_r < -800\text{m}$. Fig. 2 illustrates that data beyond this rectangle are dropped from the query. We obtained queries for every runway for the entire week. We transform the time stamp of each of these outputs to second-format with respect to a time reference. We consider 12am on January 1, 2003 as time zero.

Position is recorded at a second rate; however, there are time gaps when position is not recorded. For such cases, if the gap is at most 10 seconds, we linearly interpolate the time-position of the aircraft between two boundaries of the time gap for every second. We do not apply this interpolation for the time gaps of more than 10 seconds. This procedure is implemented in MATLAB.

We also need to attach wake vortex weight classes, and weather conditions (Instrumental Meteorological Condition IMC or Visual Meteorological Condition VMC) information to data records. In our one week sample, there are totally 1496 distinct mode-s values. For these aircraft, we managed to obtain wake vortex weight class of 93% of them, of which 67% is provided by Sensis Corporation and the rest is obtained by matching and search of tables of the FAA aircraft registration database, including MASTER, ACFTRF, and Aircraft Information tables. The weather condition for every quarter hour is reported in Aviation System Performance Metrics (ASPM) database in local time. Considering the time column of the data, we add a new column to records to indicate IMC and VMC weather condition.

After data preparation in the aforementioned manner, we now discuss how to extract samples of random variables of the

landing process, and compute desired landing statistics. Recorded data of a given aircraft might include many landings, departures, or fly-overs, but these operations are not differentiated in the database. We now introduce an algorithm to distinguish landings from other operations, and to calculate samples of *LTI*, *IAD*, and *ROT* samples.

B. Algorithm to Extract Samples

The procedure should recognize landings then extract necessary records through the following steps:

1. For each mode-s, divide all records of a single aircraft into separate operations (landings, departures, etc). We suppose that a new operation begins whenever there is a time gap of more than 15 minutes between any two records of that aircraft. Any of these operations might be a landing, departure, fly over, or a ground operation.
2. Check if a given operation is a landing on a given runway, 21L for example, by checking if it passes the following tests:
 - Let t_{\min} and t_{\max} be the first and last times for which the aircraft is in the “query box.”
 - If $X(t_{\min}) - X(t_{\max}) > 5,000$ m, then the aircraft proceeds from right to left, and has been long enough in the runway direction to be a candidate for a landing on runways 21L, 21R, 22L, 22R, 27L, or 27R. Similarly, if $X(t_{\min}) - X(t_{\max}) < -5,000$ m, then it is a candidate for a landing on runways 03R, 03L, 04R, 04L, 09R, or 09L.
 - Check if the aircraft ever crosses the threshold of the specific runway and is observed over the runway
3. Repeat step two for all operations and aircraft, and record their threshold time and location. Record the time and location of aircraft when it is first observed outside of the runway rectangle after landing, i.e. taxi-in time and

TABLE I
NUMBER OF PEAK TIME LANDINGS OBSERVED FROM FEB2, 2003 TO FEB8, 2003

a/c Type	Runway												Total	%
	03L	03R	04L	04R	09L	09R	21L	21R	22L	22R	27L	27R		
Not Available	-	1	3	-	-	-	11	0	0	7	1	2	26	1.4
Small	-	19	26	-	-	-	98	0	3	101	18	17	280	15.1
Large	-	96	158	-	-	-	445	1	18	483	107	111	1418	76.2
B757	-	8	15	-	-	-	39	0	0	51	5	11	129	6.9
Heavy	-	0	4	-	-	-	1	0	1	1	0	0	7	0.4
Total	0	124	206	0	0	0	594	1	22	643	131	141	1862	100

location. If the aircraft track disappears over the runway, then exit from runway is not recorded, record zero or blank for the exit time.

- Sort landings in ascending manner, to recognize follow-lead aircraft. Record the location of any follow aircraft at the moment its lead crosses the runway threshold.
- Calculate *ROT* for any aircraft, and *LTI*, and *IAD* for any pair of lead-follow aircraft. ■

Depending on the objective of a study, observations shall be classified based on weather condition, weight class of follow-lead aircraft, arrival rate, etc.

III. LANDING STATISTICS

We define a peak period for a given runway to be a quarter-hour with at least seven landings on that runway. For the week Feb 2, 2003 to Feb 8, 2003 we observed 1862 peak period landings out of 4313 landings observed for the entire week on all twelve runways. Peak period landings are distributed among runways and aircraft types as shown in Table I. The majority of these landings occur on runways 21L and 22R. Only 1.4% of wake vortex weight classes of peak period landings could not be recognized.

Fig. 3 shows arrival rates per quarter hour for runway 21L. The horizontal axis is in local time. Observations start at 7:00pm Feb 1, 2005. Shaded periods over the time axis indicate IMC periods for the airport. The arrival pattern for runway 22R is similar to this one since the arrival traffic is equally directed to these two parallel runways whenever these runways are in the landing configuration.

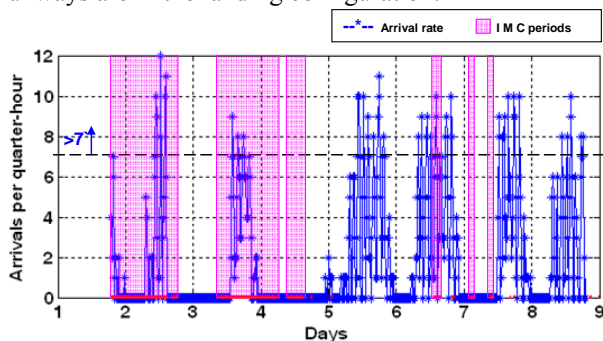


Fig. 3. Arrival rate to runway 21L from late Feb 1 to 8, 2003 local time

To double check completeness of observations in the multilateration database and to validate our data preparation and sample extraction algorithm, we compared the number of

landings reported in ASPM database with the results from our study. The comparison plot is given in Fig. 4. Overall for this week, ASPM reports 160 more landings than ours. This corresponds to a small proportion of 3.6% ($=100*160/4473$) of ASPM records. Average and standard deviation of “Observed minus ASPM” rates are 0.24 and 1.7 arrivals per quarter-hour, respectively. This difference can be the result of missing mode-s and unrecorded landings that might have happened because of off transponders or non-transponder aircraft.

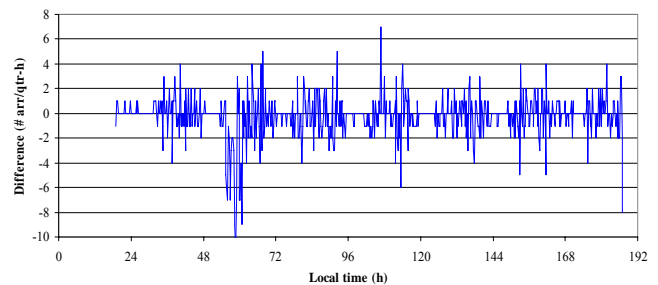


Fig. 4. (Observed – ASPM) per qtr-h arrival rate. The mean and standard deviation are 0.24 and 1.7 arr/qtr-h, respectively.

To analyze system operations it is also important to know the proportion of follower-leader aircraft pairs. Table II shows this proportion for our data (peak times only), which is also called a transition matrix. About 59% of the landings are L-L aircraft. In 77.1% and 77.3% of the times a large aircraft was

TABLE II
FOLLOW-LEAD AIRCRAFT TRANSITION MATRIX (% OUT OF 1805 PAIRS) IN PEAK PERIODS

Follow \ Lead	Small	Large	B757	Heavy	Sum
Small	1.7	12.5	1.2	0.1	15.5
Large	12.8	58.8	5.4	0.3	77.3
B757	0.9	5.4	0.6	0.0	6.9
Heavy	0.1	0.3	0.0	0.0	0.4
Sum	15.5	77.1	7.1	0.3	100

In 59% of landings a large aircraft follows another large one. In 77% of the time a large aircraft is the following (the leading) one.

the lead and the follow aircraft, respectively.

A. Peak time ILS Landing Probability Distributions

In risk and capacity analysis, the pattern of the approach process behavior in peak periods is of interest. For this reason, we focus on periods during which there are seven or more

landings per quarter hour. Also, the approach process under IMC is the subject of sampling and distribution estimation in this paper.

Table III is the default standard for the “approach in-trail threshold separation minima” under Instrument Flight Rule (IFR) put forth by Federal Aviation Administration. We are interested to know what the probability distributions of *LTI* and *IAD* are for class of follow-lead aircraft with the 3 nmi separation spacing minima indicated in Table III, i.e. pairs S-S, L-S, B757-S, H-S, L-L, B757-L, and H-L. In specific situations, 3 nmi spacing standard may be reduced to 2.5 nmi [12]-[13]. However, differentiating these situations is not the subject of this paper.

TABLE III
IFR APPROACH IN-TRAIL THRESHOLD SEPARATION MINIMA (NMI)

Follow a/c	Lead a/c			
	Small	Large	B757	Heavy
Small	3	4	5	6
Large	3	3	4	5
B757	3	3	4	5
Heavy	3	3	4	4

We have obtained 511 samples of *IAD* and 523 samples of *LTI* for the class of pairs of interest. Independence of samples is examined by “one-lag scatter plot” in Fig. 5 for *IAD*; for more information on statistical concepts discussed in this paper see, e.g., [14]-[16], for example. The plot does not demonstrate a specific pattern of dependency among the samples and one-lag correlation coefficient is 0.25. Higher degrees of lags have lower correlation coefficients. Thus independence of *IAD* samples, which is required for distribution fitting purposes, is accepted. In the same manner, we conclude independence of *LTI* samples by examining the one-lag scatter plot with related correlation coefficient of 0.25.

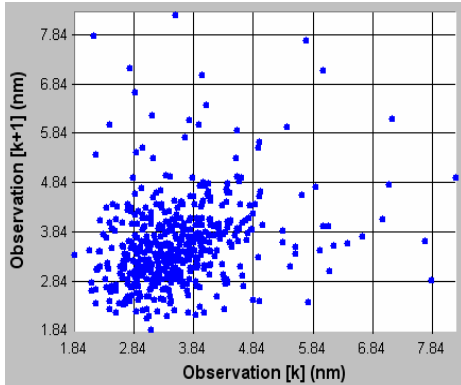


Fig. 5. The one-lag scatter plot of peak-IMC period *IAD* of pairs with 3 nmi separation standard (511 samples). The one-lag correlation coefficient is 0.25. Correlation coefficients for higher degrees of lags are smaller.

We presented histograms and probability distribution function (PDF) fits for *IAD* and *LTI* in Fig. 6 and Fig. 7 with increments of 0.5 nmi and 15 s, respectively. For practicality, in fitting a distribution, we limit *IAD* to a minimum of 1.5 nmi and estimate its distribution by Erlang(1.5;0.35,6) where the values represent location (shift), scale, and shape parameters, respectively. The mean of the Erlang distribution is [(location par.)+ (shape par.)*(scale par.)], and the variance is [(shape par.)*(scale par.)²]. We use the Maximum Likelihood Estimation (MLE) method for this estimation and for

estimations of *LTI* and *ROT* probability distributions. The fit passes Kolmogorov-Smirnov test (KS-test) for significance levels less than 0.10. The Log-Logistic(1.5;1.9,4.5) distribution provides a slightly better fit where values represent location, scale, and shape parameters, respectively.

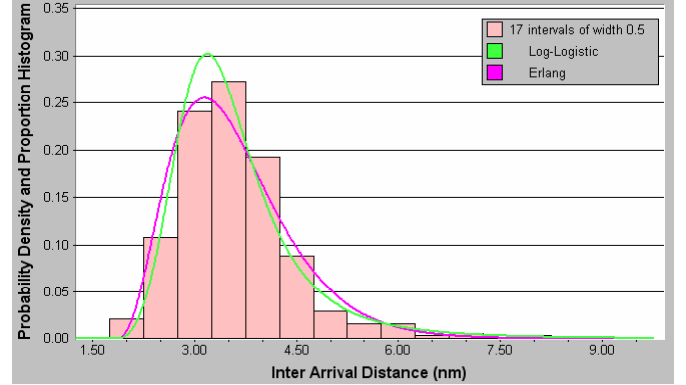


Fig. 6. *IAD* histogram and distribution fits for 511 samples. Sample mean is 3.6 and standard deviation is 0.88 nmi. Erlang(1.5;0.35,6) fit has the mean 3.6 and standard deviation 0.86 nmi.

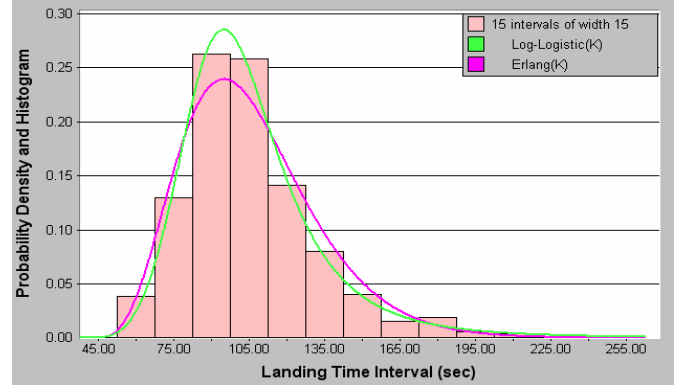


Fig. 7. *LTI* histogram and distribution fits for 523 samples. Erlang(40;11,6) has the mean 106 and standard deviation 27 seconds.

We estimated probability distribution of *LTI* by Erlang(40;11,6) when we enforce minimum of 40 seconds. Similar to the *IAD* case, the Log-Logistic(40;61,4.4) distribution provides a slightly better fit than Erlang distribution, which is a specific case of the gamma distribution. The Erlang fit is accepted by KS-test for significance levels of 0.05 or smaller.

We have obtained 669 samples of *ROT* in peak IMC periods. We conclude that they are independent because the *N*-lag correlation coefficient, $N=1, 2, \dots$, is less than or equal to 0.08; also the one-lag scatter plot does not show any specific pattern of relationship. The histogram and two distribution fits for *ROT* samples are shown in Fig. 8. We estimate the distribution of *ROT* using three different distributions – gamma, beta, and normal. Using the MLE method, the best fits are Gamma(25;2.8,8.5) in the enforced range of (25,∞) s, Beta(25,110;6.1,15.4) in the enforced range of (25,110) s, where 3rd and 4th values represent shape parameters, and $N(49,8.1^2)$ in the open range of $(-\infty, \infty)$. Gamma is the best fit among these three with the maximum likelihood criterion; however, the beta distribution might be preferred because, as in real situations for *ROT*, it has lower and upper bounds (for example it can not be negative). The normal distribution, which is used in [3]-[5], is rejected for *ROT* samples in the 0.1 significance level. Mean and variance

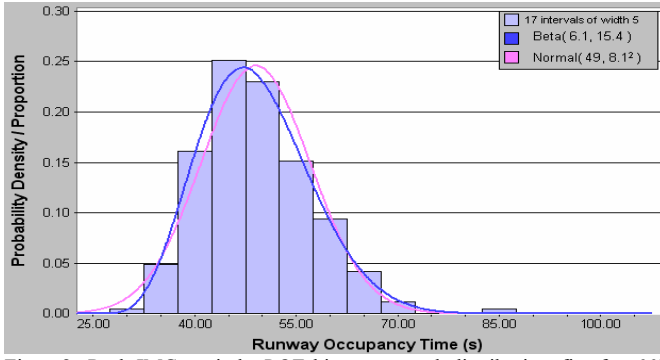


Fig. 8. Peak-IMC periods *ROT* histogram and distribution fits for 669 samples for all aircraft types. Sample mean and standard deviation are 49.1, and 8.1 s. Beta(25,110;6.1,15.4) fit has the mean 49.1, and standard deviation 8.1 s.

of Beta($L, U; \alpha, \beta$) are

$$\begin{cases} \mu = L + \frac{1}{U-L} \cdot \frac{\alpha}{\alpha + \beta} \\ \sigma^2 = \left(\frac{1}{U-L} \right)^2 \cdot \frac{\alpha \cdot \beta}{(\alpha + \beta)^2 (\alpha + \beta + 1)} \end{cases}$$

We also want to know if *ROT* is different under IMC and VMC weather conditions. Fig. 9 shows histograms of *ROT* under VMC and IMC for the runways with similar taxiway configurations, i.e. 21L/03R and 22R/04L. The structure of runways 27L and 27R seems to be different from 21L/03R and 22R/04L, as also seen in Table IV.

Visual inspection of the figure does not suggest any

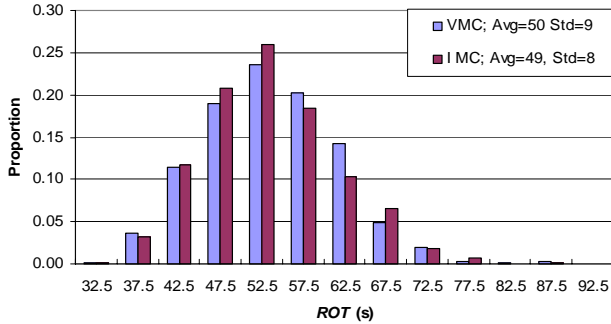


Fig. 9. Histogram of *ROT* under VMC (895 samples) vs. IMC (590 samples) for runways 21L/03R and 22R/04L. We can not observe significant difference between IMC and VMC samples.

significant difference between IMC and VMC *ROT* for this week of data. (Here, IMC / VMC is only distinguished by the corresponding flag in the ASPM database. We have not conditioned on other complementary variables, like surface visibility, which might also affect *ROT*. Thus, data from a different week in which surface visibility is reduced might show a distinction between IMC / VMC.) From the data, the average and standard deviation of *ROT* in VMC are 50 s, and 9 s, respectively. In IMC, the average and standard deviation are 49 s, and 8 s.

Also of interest is the probability (or frequency) that the *LTI* between two consecutive aircraft is less than the *ROT* of the leading aircraft. We represent this probability by $P\{LTI_{k,k+1} < ROT_k\}$, $k=1, 2, \dots$, and name it “runway-related approach risk.” Fig. 10 shows pairs of observations ($LTI_{k+1,k}$, ROT_k) observations which is the *ROT* of the lead aircraft k versus the

Runway	Statistic	VMC	IMC
03R	N	60	30
	Range (s)	[33,68]	[32,64]
	Avg (s)	48	47
	Std (s)	7	8
04L	N	63	91
	Range (s)	[40,60]	[39,68]
	Avg (s)	48	49
	Std (s)	6	6
21L	N	271	148
	Range (s)	[31,70]	[29,72]
	Avg (s)	45	48
	Std (s)	8	10
22L	N	22	-
	Range (s)	[40,79]	-
	Avg (s)	55	-
	Std (s)	9	-
22R	N	283	171
	Range (s)	[26,72]	[39,70]
	Avg (s)	53	50
	Std (s)	6	6
27L	N	60	38
	Range (s)	[38,58]	[39,60]
	Avg (s)	48	48
	Std (s)	5	5
27R	N	72	26
	Range (s)	[38,105]	[36,84]
	Avg (s)	57	54
	Std (s)	12	11
Total	N	828	504
	Range (s)	[26,105]	[29,84]
	Avg (s)	49	49
	Std (s)	8	8

Overall, from this table, we can not observe significant difference between *ROT* under IMC and VMC. Based on the sample, runway 27R has higher mean and variability than other runways.

LTI between aircraft k and $k+1$ for peak period landings. We have limited *LTI* in the figure to 200 seconds for the purpose of clarity. In this figure, there are two observations having *ROT* of 105 s which correspond to landings on runway 27R in VMC. They are exceptional cases since they are far from other sample population and we consider them as outliers. They are 19 s bigger than the second largest sample 86 s, for example.

Fig. 10 also demonstrates independence of $LTI_{k,k+1}$ and ROT_k , for all k . The Kendall “sample-correlation statistic,” which measures dependency in non-parametric statistics, is 0.085 and supports independence of these random variables; for more discussion on this parameter see [16]. The sample correlation coefficient is 0.15 and also confirms the independence hypothesis.

Now we provide an empirical and a theoretical “point estimation” for $P\{LTI_{k,k+1} < ROT_k\}$, $k=1, 2, \dots$, in peak periods

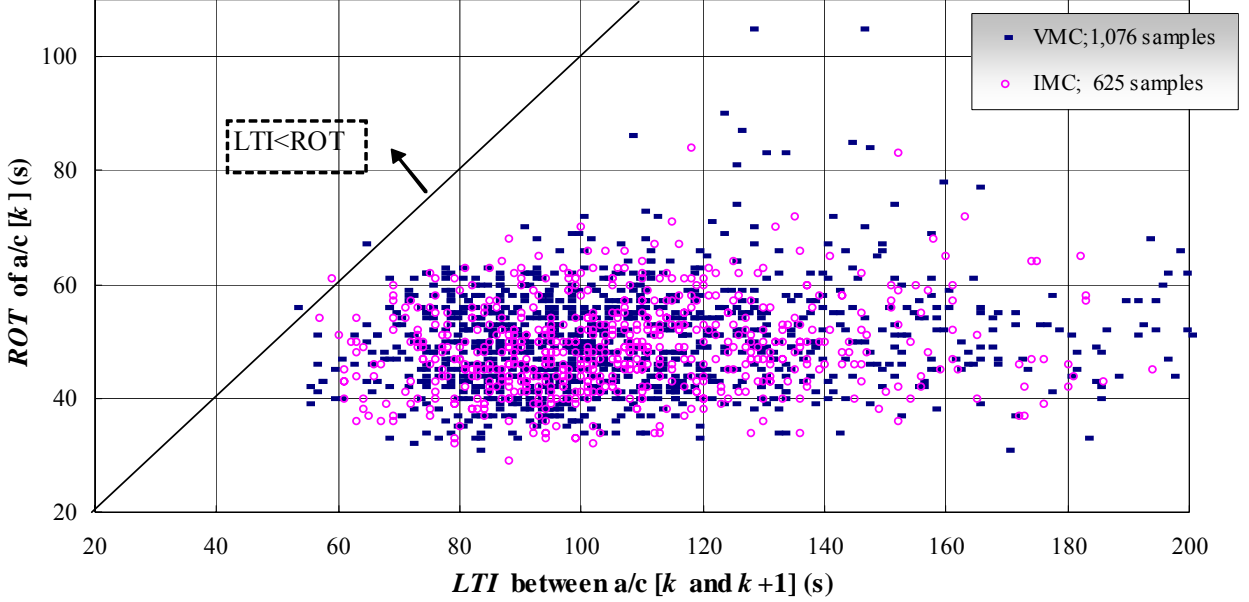


Fig. 10. Runway Occupancy time of aircraft k , ROT_k , versus Landing Time Interval between aircraft k and $k+1$, $LTI_{k,k+1}$. In this figure, pairs of follow-lead aircraft are not differentiated based on their weight class. For three points above 45 degree line, $LTI_{k,k+1}$ is less than ROT_k one of which has occurred under IMC.

for pairs of aircraft with separation standard 3 nmi in table III.

1) *Empirical Method*: There are three points above the 45 degree line. These points represent events where $LTI_{k,k+1} < ROT_k$. The sample frequency is 0.0016 with respect to 1862 peak period landings. (Out of 1862 landings, there were 108 landings for which we could not obtain the ROT due to disappearance of the aircraft track over the runway. This might be because the aircraft turned off the transponders or for other reasons. 44 of these lost data happened in IMC and 64 in VMC. We assume that these landings would not have been above the 45 degree line in the figure.)

The frequency of $LTI_{k,k+1} < ROT_k$, for $k=1, \dots, 4312$, is 0.0007 - that is, 3 out of 4313 landings, assuming that no such event occurred in non-peak periods. As shown in Fig. 10, for 1 (for 2) out of 625 IMC (1076 VMC) landings we have $LTI_{k,k+1} < ROT_k$, i.e. the estimated probability of 0.0016 (0.0019).

2) *Theoretical method*: We use the probability distribution fits that we calculated as $ROT \sim \text{Beta}(6.1, 14.5)$ in the range (25, 110), and $LTI \sim \text{Erlang}(40; 11, 6)$ to estimate $P\{LTI < ROT\}$. Fig. 11 shows the overlap of these probability distributions. Because there is an overlap between LTI and ROT , then $P\{LTI < ROT\}$ is positive. We note that in fitting the PDF for LTI , we have not considered samples of LTI that we could not obtain their corresponding ROT . Let $g_{ROT}(\cdot)$ represent PDF of ROT , and $F_{LTI}(\cdot)$ represent Cumulative Density Function (CDF) of LTI . Then,

$$\begin{aligned} p\{LTI < ROT\} &= \int_{-\infty}^{\infty} p\{LTI < ROT | ROT = x\} \cdot g_{ROT}(x) dx \\ &= \int_{25}^{110} p\{LTI < x\} \cdot g_{ROT}(x) dx \\ &= \int_{25}^{110} F_{LTI}(x) \cdot g_{ROT}(x) dx. \end{aligned} \quad (4)$$

Equation (4) cannot be evaluated analytically for the distributions we have chosen. We estimate (4) using stochastic

simulation. The result is 0.004, as a point estimation for the pairs of interest in peak-IMC period. ■

We see that the theoretical estimation 0.004 is about 2.5

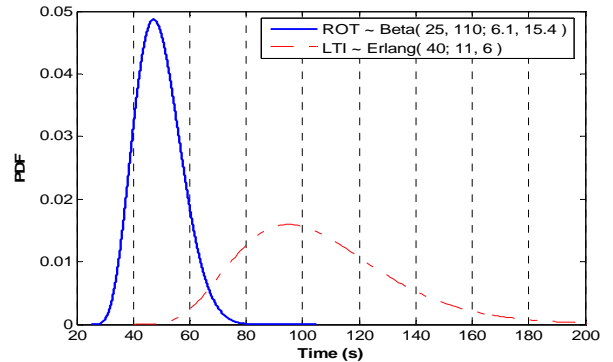


Fig. 11. Overlap of ROT and LTI . We obtain point estimation 0.004 for $P\{LTI < ROT\}$. The estimation would be slightly smaller if we chose logistic distribution for LTI .

times of the empirical estimation 0.0016 for peak-IMC periods. We shall note that these estimations are optimistic firstly because we have missed about 3.5% of total landings based on the ASPM, and secondly we could not obtain ROT for 44 out of 669 peak-IMC landings. These two effects may have added to $P\{LTI < ROT\}$, i.e. may have had bigger LTI than ROT of their leading aircraft.

IV. CONCLUSIONS

We presented an efficient way to use multilateration surveillance system data taking into account and analyzing noise, errors, and missing data. We obtained the wake vortex weight class of 98.6% of aircraft landing in peak periods. We added this information to the multilateration data along with the meteorological conditions that we obtained from the ASPM database. We gave an algorithm to extract samples of

random variables *LTI*, *IAD*, and *ROT* from the data. The samples were conditioned on IMC times and peak traffic periods in which there were seven or more landings per quarter hour on a given runway. Also, *LTI* and *IAD* were additionally conditioned based on follower-leader wake vortex weight class and aggregated for ones with a minimum separation standard of 3 nmi – namely, pairs S-S, L-S, B757-S, H-S, L-L, B757-L, and H-L.

The data supported our assumption that samples of each random variable were independent. We represented the PDF of *LTI*, *IAD*, and *ROT* by a few known density functions and compared their performance. Fitting distributions to the collected samples showed that *ROT* is best represented by a beta distribution, but not with a normal distribution, which is generally assumed in the literature. *LTI*, and *IAD*, for the F-L pairs of under study, were best fit by log-logistic distributions; however, Erlang (gamma) distribution was also accepted for these random variables. We preferred to use the Erlang distribution rather than the log-logistic distribution because it is better known and has enough accuracy to represent behavior of *LTI* and *IAD*. We also showed that *LTI* between the leading and following aircraft is independent of *ROT* of the leading one. Our overall observations suggested that there was almost no difference of *ROT* between IMC and VMC conditions, for the particular week observed at DTW. We estimated the probability (or frequency) of *LTI*<*ROT* in peak-IMC periods with empirical and theoretical calculations.

Investigation of data for longer time periods, e.g. one month, and for a visual landing system (VFL) at this airport and other airports can be the subject of future studies. Providing methodologies to incorporate incomplete data of (*LTI*, *ROT*) with missing *ROT* in estimation of “runway-related risk” can be a research problem. Distribution of other random variables in the approach process, such as time between exits from the runway, and inter arrival times to the terminal radar approach control (TRACON) area, are subjects for future research.

DISCLAIMER

This paper solely represents the opinions of the authors and does not necessarily reflect the opinion of the United States government or NASA.

ACKNOWLEDGEMENT

The authors would like to thank Wayne Bryant, Wake Program Manager at NASA Langley, for support of this research. We also thank the Volpe National Transportation Systems Center and Sensis Corporation for help in acquiring, manipulating, and understanding the multilateration data. We would like to thank Dr. George Donohue for helpful comments and insights on this research.

REFERENCES

- [1] B. Levy, J. Legge, and M. Romano, “Opportunities for improvements in simple models for estimating runway capacity,” presented at the 23rd Digital Avionics Systems Conference, Salt Lake City, UT, October 2004.
- [2] C.R. Haynie, “An investigation of capacity and safety in near-terminal airspace for guiding information technology adoption,” Ph.D.

- dissertation, Dept. Sys. Eng. and Oper. Res., George Mason Univ., Fairfax, VA, 2002.
- [3] Y. Xie, J. Shortle, G. Donohue, “Runway landing safety analysis: a case of Atlanta Hartsfield airport,” presented at the 2003 Digital Avionics Systems Conf., Indianapolis, IN, 2003.
- [4] Y. Xie, J. Shortle, P. Choroba, “Landing safety analyses of an independent arrival runway,” presented at the 2004 Int. Conf. for Res. In Air Trans., Zillina, Slovakia.
- [5] Y. Xie, “Quantitative analysis of airport runway capacity and arrival safety using stochastic methods,” Ph.D. dissertation, Dept. Sys. Eng. and Oper. Res., George Mason Univ., Fairfax, VA, 2005.
- [6] Ballin, M.G., H. Erzberger, “An analysis of landing rates and separations at the Dallas/Fort Worth International Airport,” NASA, Tech. Memo. 110397, July 1996.
- [7] H.F. Vandevenne, and M.A. Lippert, “Using maximum likelihood estimation to determine statistical model parameters for landing time separations,” 92PM-AATT-006, March 2000
- [8] J.W. Andrews, and J.E. Robinson, “Radar-based analysis of the efficiency of runway use,” AIAA Guidance, Navigation, and Control Conf., Quebec, August 2001
- [9] J. Rakas, H. Yin, “Statistical modeling and analysis of landing time intervals: case study of Los Angeles International Airport, California,” Transportation Research Record: Journal of the Transportation Research Board, No. 1915, 2005, pp. 69-78.
- [10] FAA Airport Diagram, AL-119, 16 Feb 2006, Available <http://204.108.4.16/d-tp/0602/00119AD.PDF>
- [11] B. Jeddi, “Preliminary Exploration of DROMSIV data on Detroit Airport (DTW),” CATSR Internal report, August 2004
- [12] FAA Order 7110.65, Air Traffic Control., Federal Aviation Administration, Sept. 1993, Wake Turbulence, Para 2,1,19
- [13] FAA Order 7110.65, Same Runway Separation, Federal Aviation Administration, Sept. 1993, Wake Turbulence, Para 3,9,6
- [14] A.H. Bowker, and G.J. Lieberman, *Engineering Statistics*, 2nd Ed, Prentice-Hall, Inc, 1972.
- [15] A.M. Law, *ExpertFit: user’s guide*, Averill M. Law & Associates, 2000
- [16] M. Hollander, D.A. Wolf, *Nonparametric Statistical Methods*, 2nd Ed., John Wiley & Sons, Inc., 1999.

Babak G. Jeddi (B.S.’93–M.S.’96 and ’03) is a Ph.D. candidate in the Department of Systems Engineering and Operations Research, and a research assistant in the Center for Air Transportation Systems Research at George Mason University. His experience includes quality and productivity improvement in manufacturing and service organizations. His research interests include analysis of supply chain and air transportation systems via stochastic processes, simulation, and network modeling. He received his masters’ degree in Industrial Engineering from University of Cincinnati, Ohio, US.

John F. Shortle, Ph.D., is an assistant professor of Systems Engineering at George Mason University. His experience includes developing stochastic, queuing, and simulation models to optimize networks and operations. His research interests include simulation and queuing applications in telecommunications and air transportation. He received his doctorate degree in operations research from University of California at Berkeley, California, US.

Lance Sherry, Ph.D., is an associate research professor, and executive director of the Center for Air Transportation Systems Research at George Mason University. His research interests include productivity improvement, strategic planning, and dynamic systems. He received his doctorate degree in Industrial Engineering from Arizona State University, Arizona, US.